Supplemental information for

Cyclic LIN-42/PERIOD precisely times stage-specific cell migration through gene circuit dynamics

Yi-Chen Chen[1,2], Yi-Ting Cheng[3], Min-Ren Chiang[3], Ching-Cher Sanders Yan[2], Chun-Yi David Lu[1], Arthur D. Lander[4*], Yi-Chun Wu[3,6,7*] and Chao-Ping Hsu[2,5,8*]

1. Department of Chemistry, National Taiwan University, Taipei, Taiwan.
2. Institute of Chemistry, Academia Sinica, Taipei, Taiwan.
3. Institute of Molecular and Cellular Biology, National Taiwan University, Taipei, Taiwan.
4. Department of Developmental and Cell Biology and Center for Complex Biological Systems, University of California, Irvine, Irvine, California, United States of America.
5. Physics Division, National Center for Theoretical Sciences, Taipei, Taiwan
6. Institute of Atomic and Molecular Sciences, Academia Sinica, Taipei, Taiwan.
7. International Graduate Program of Molecular Science and Technology, National Taiwan University, Taipei 10617, Taiwan
8. Genome and Systems Biology Degree Program, National Taiwan University, Taipei 10617, Taiwan

*Corresponding authors. Email: adlander@uci.edu (A.D.L.); yichun@ntu.edu.tw (Y.-C.W.); cherri@as.edu.tw (C.-P.H.)

Table of contents

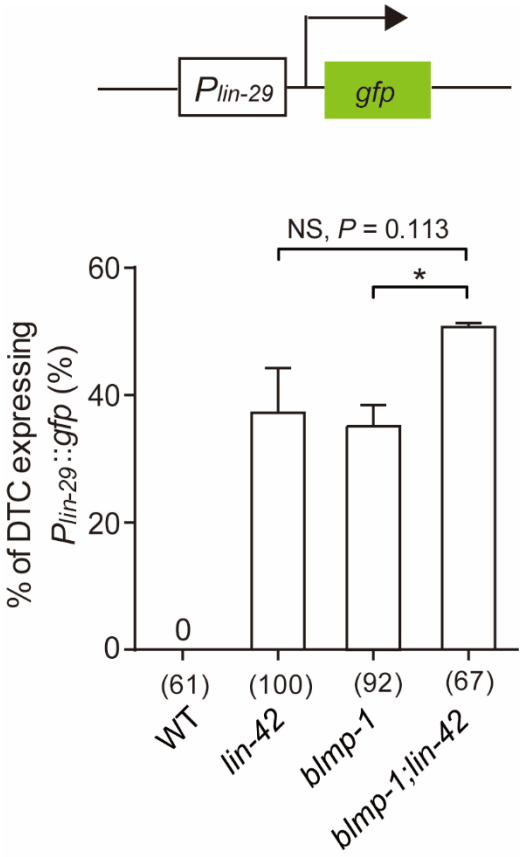

Figure S1 *lin-42* regulates *lin-29* transcription in the wild-type worm.

(A) Percentage of wild-type and *blmp-1* mutant worms with distal tip cells (DTCs) expressing the $P_{lin\text{-}29}$*::gfp* transgene from L2 to mid-L3 stage, with or without *lin-42* RNAi treatment. A schematic diagram of the $P_{lin\text{-}29}$*::gfp* transcriptional reporter is shown on the top. Numbers in parentheses indicate numbers of worms scored. Data shown are mean ± s.e.m. *p<0.05, NS, no statistical significance. Fisher's exact test. Alleles or treatment used: *blmp-1*(*s71*), *lin-42*(*RNAi)*.

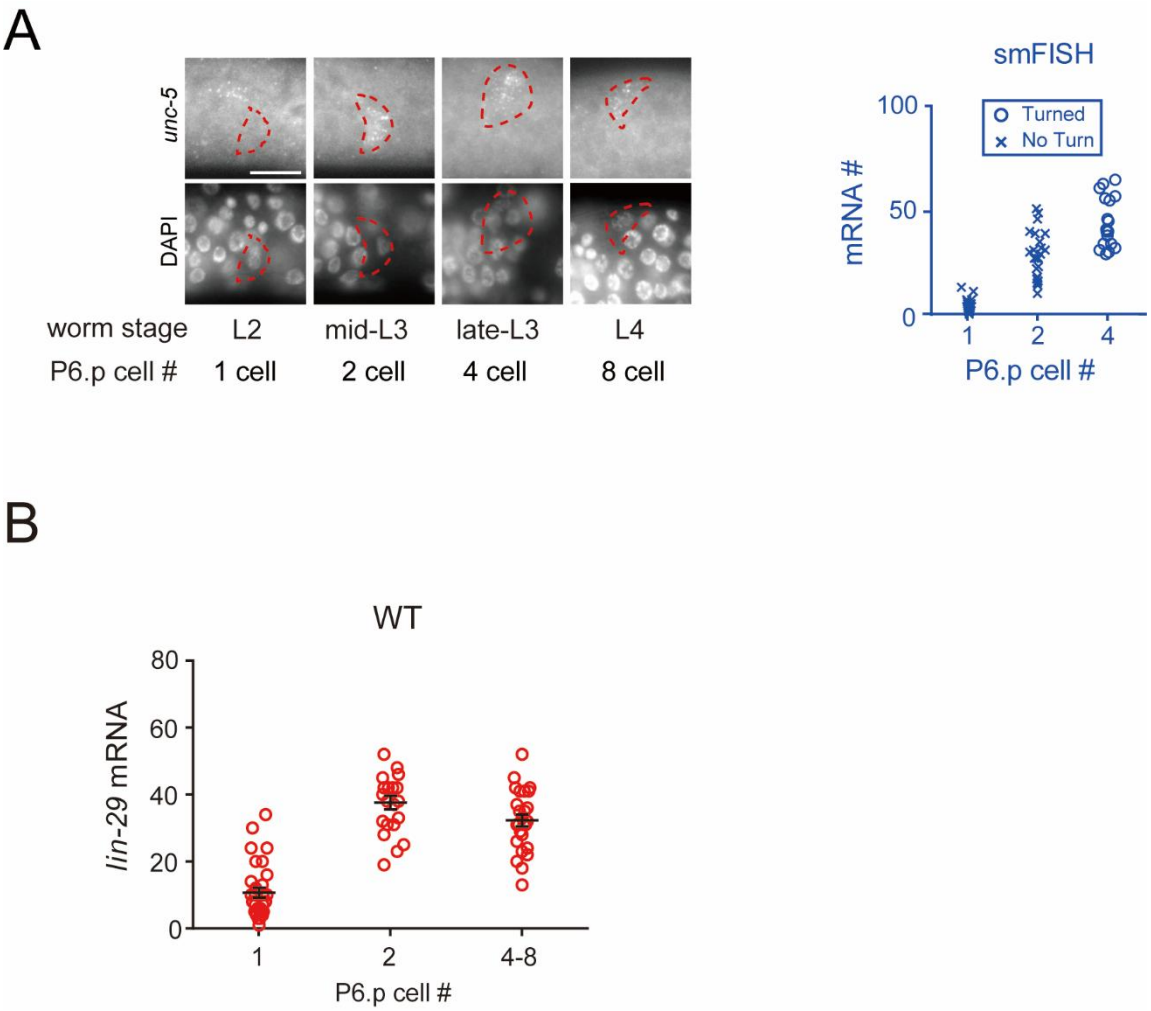

Figure S2 *unc-5* and *lin-29* transcript levels measured by single molecule fluorescence in situ hybridization (smFISH) in the wild-type worm.

(A) (left) Representative *unc-5* smFISH (upper) and DAPI (lower) images of the wild-type posterior gonadal arms at the indicated developmental stage. The DTC was identified based on its position and the DAPI staining. The red dashed line indicates the boundaries of the posterior DTC. (right) *unc-5* transcript levels measured using smFISH (right and blue, n=19, 26, 23 for 1-, 2- and 4-P6.p cell stages, respectively), at the indicated division stage of the P6.p. cell.
(B) *lin-29* transcript level measured by smFISH at the indicated P6.p cell division stage in the wild-type worm. Each circle represents the amount of the *lin-29* transcript detected in one posterior DTC. n=34, 24, 29 for the 1-, 2- and 4-8-P6.p cell stage. The black bars shown are mean ± s.e.m.

A

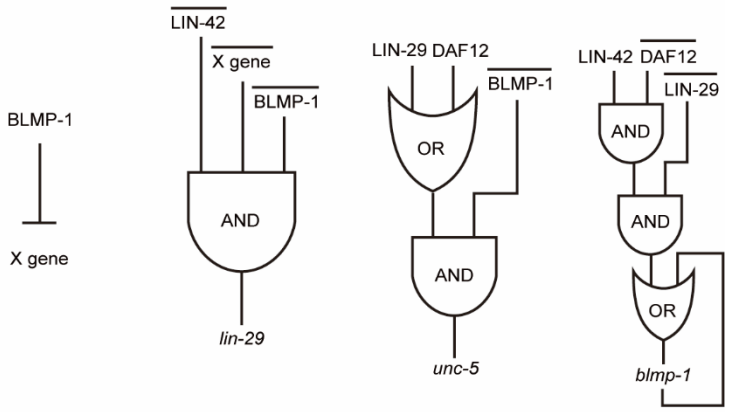
BLMP-1
X gene
LIN-42
X gene
BLMP-1
AND
lin-29
LIN-29 DAF12
BLMP-1
OR
AND
unc-5
LIN-42 DAF12
LIN-29
AND
AND
OR
blmp-1

B

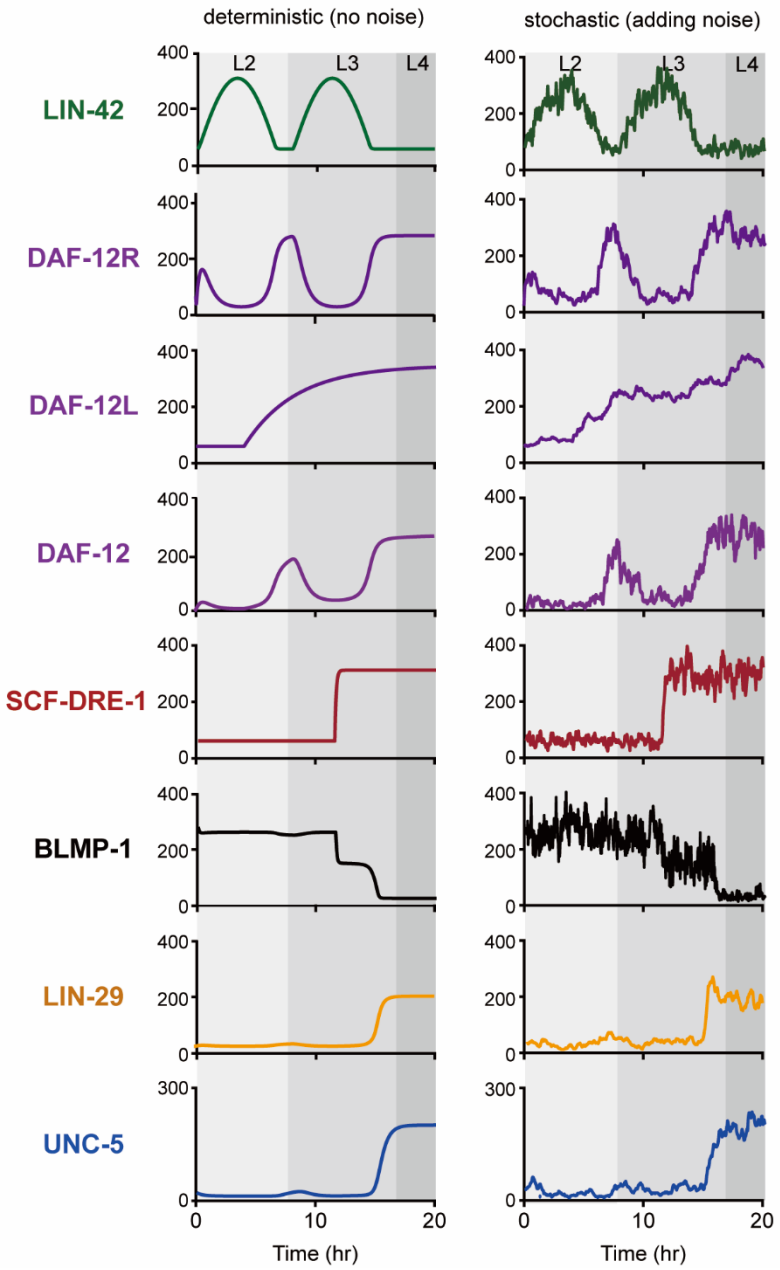
deterministic (no noise)
stochastic (adding noise)
L2
L3
L4
LIN-42
DAF-12R
DAF-12L
DAF-12
SCF-DRE-1
BLMP-1
LIN-29
UNC-5
400
200
0
300
0
10
20
Time (hr)

Figure S3 Mathematical modeling of UNC-5 expression in wild type worms

(A) Logic of combinatorial regulation employed in the mathematical model. The input genes are shown on the top and the output gene at the bottom in each diagram. A bar over an input gene name indicates negative regulation (repression), while no bar indicates positive regulation (activation) of the output gene. 'AND' or 'OR' logic describes the relationship in combinatorial regulation of the output gene. AND logic indicates both regulatory inputs are required for output gene expression, whereas OR logic indicates either regulatory input is sufficient.

(B) Deterministic and stochastic simulation of UNC-5 expression in wild type worm. Dynamic trajectories that show the levels of the indicated proteins over time in wild-type worms simulated using deterministic (left) and stochastic (right) settings. DAF-12R, DAF-12L, DAF-12 represent the ligand-free DAF-12 receptor, DAF-12 ligand, and DAF-12 complex where the DAF-12 receptor is bound with ligand.

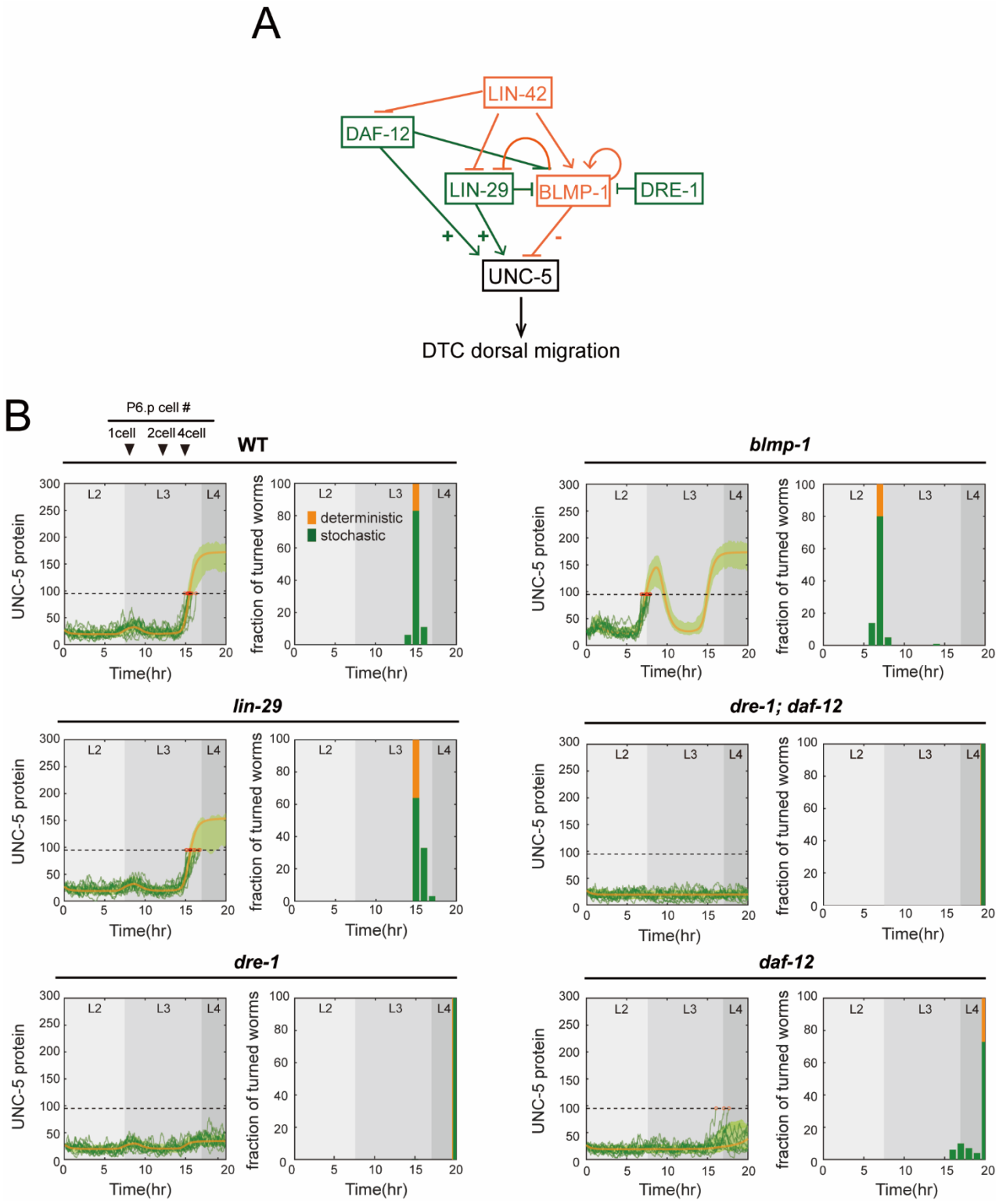

Figure S4 Simulation of DTC turning time in circuits lacking BLMP-1 activation of *lin-29*

(A) The gene regulatory circuits lacking BLMP-1 activation of *lin-29*. Genes and their interactions leading to the activation of *unc-5* expression are shown in green, and those leading to repression in orange.

(B) UNC-5 protein level (left) and distribution of DTC turning times (right) are simulated for each indicated genotype using the deterministic and stochastic models. All labels and analyses follow the same conventions as described in in Figures 2B-G.

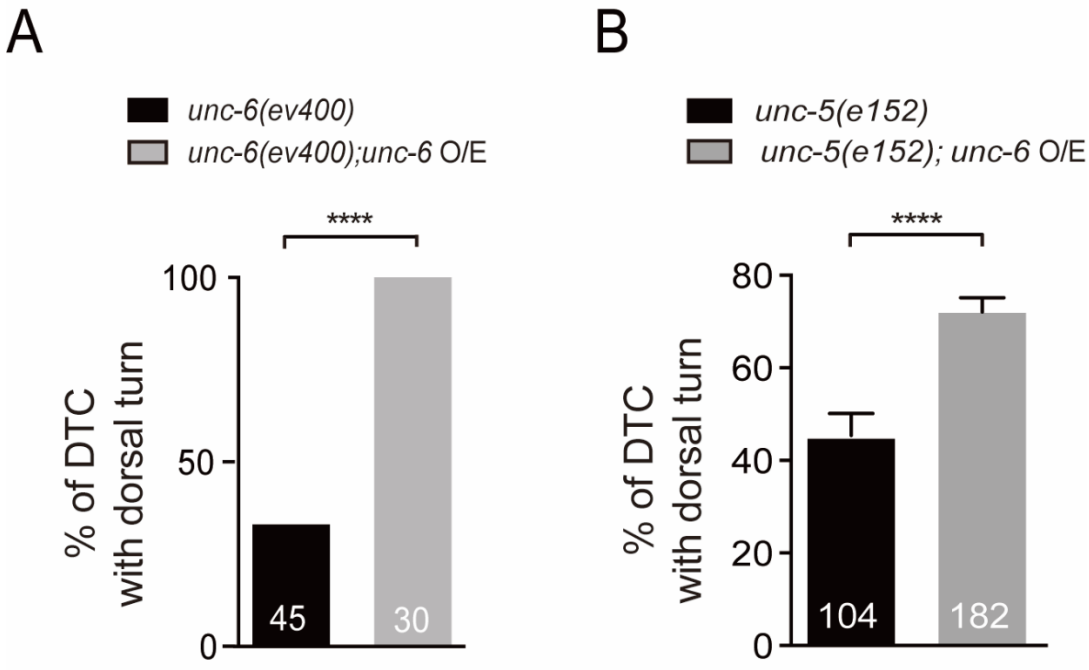

Figure S5 UNC-6/Netrin overexpression in the *unc-6(ev400)* (A) and *unc-5(e152)* (B) mutant worms

Percentage of the posterior DTCs showing dorsalward turning detected in the *unc-6(ev400)* (A) and *unc-5(e152)* (B) worms with or without the $P_{unc\text{-}6}$*::unc-6* transgene (indicated as *unc-6* O/E) at the L4 stage. Numbers inside bars indicate numbers of worms scored. Data shown are mean ± s.e.m. ****p<0.0001, Fisher's exact test.

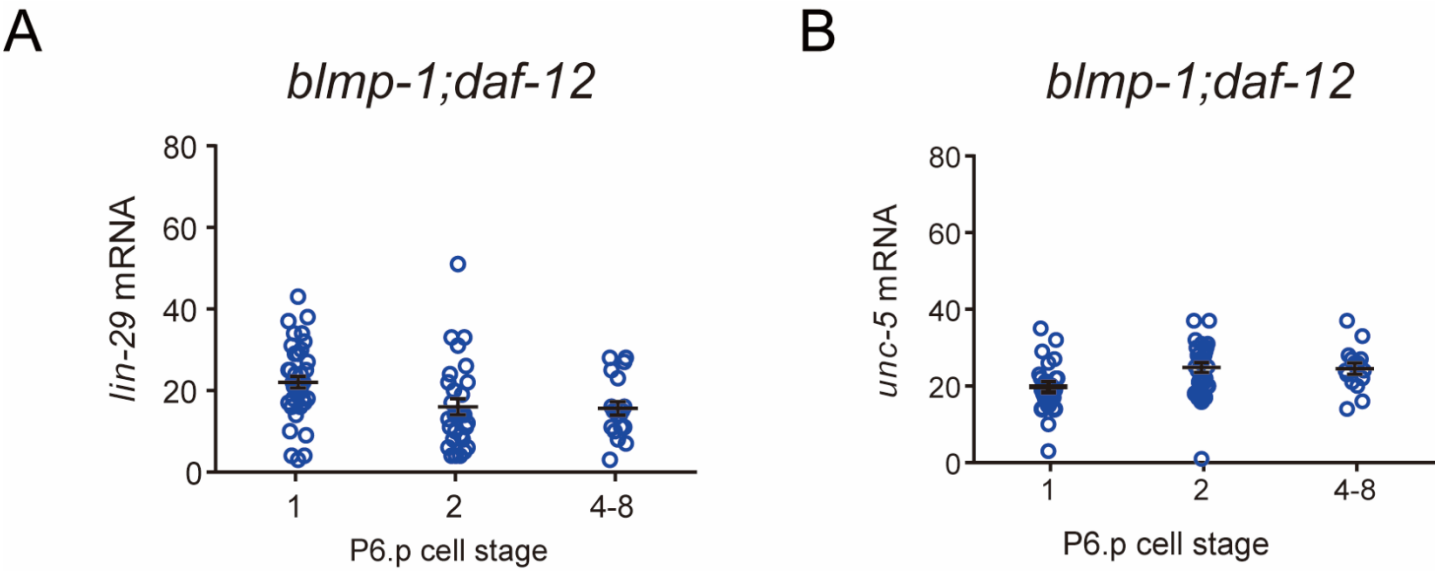

Figure S6 *lin-29* (A) and *unc-5* (B) transcript levels measured in the DTCs of the *blmp-1; daf-12* mutant

The *lin-29* (A) (n=43, 32, 22 for 1-, 2- and 4-8 P6.p cell stage) and *unc-5* (B) (n=24, 29, 33 for 1-, 2- and 4-8 P6.p cell stage) transcript levels in the posterior DTCs of *blmp-1;daf-12* mutant were measured using smFISH. Each circle represents the number of the transcript detected in one posterior DTC. Each black bar shows the mean ± s.e.m of the transcript at the indicated P6.p cell stage. Alleles used: *daf-12*(*rh64rh411*) and *blmp-1(s71)*.

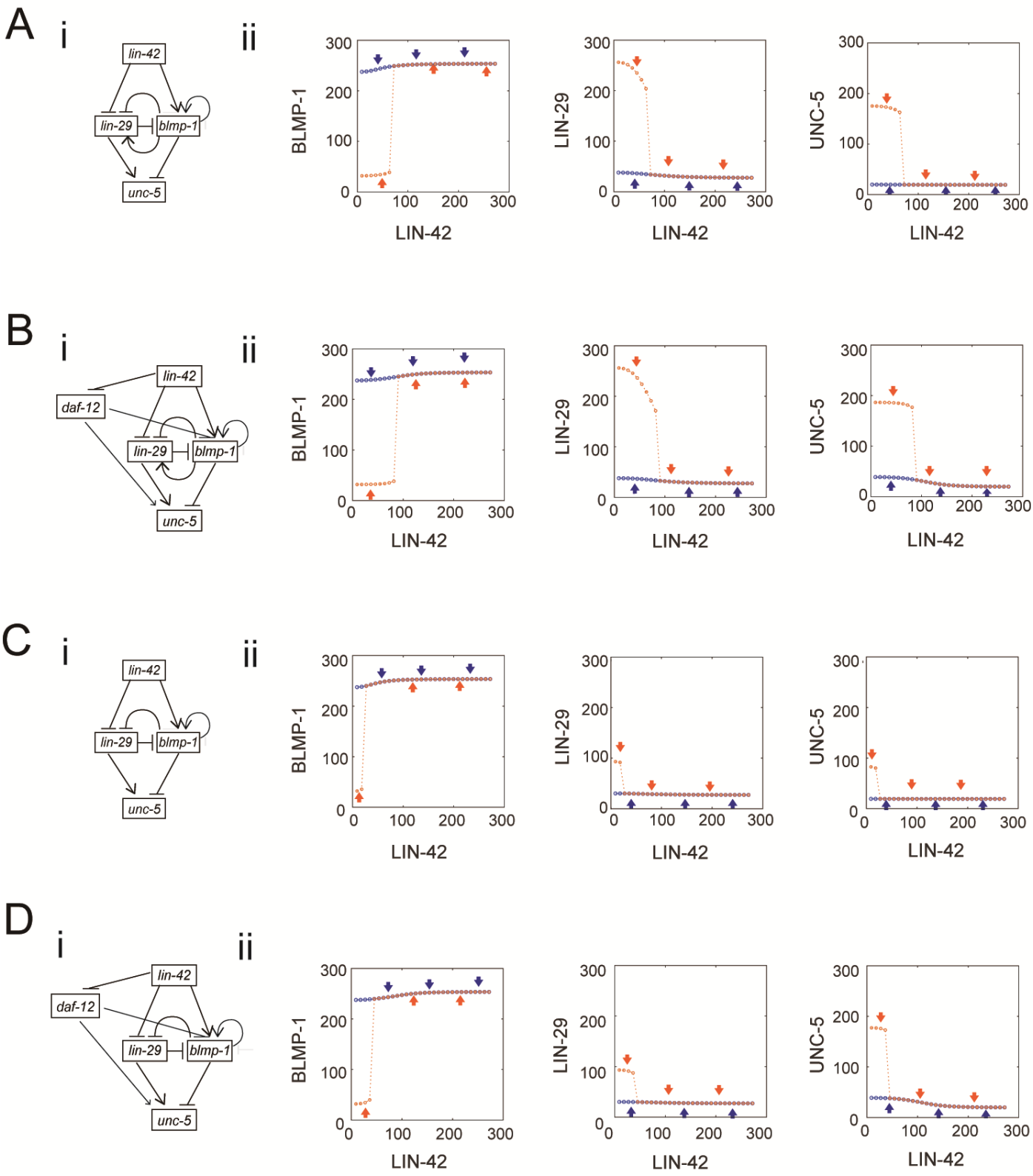

Figure S7 BLMP-1, LIN-29, and UNC-5 steady-state simulation: LIN-42 response during L2 and the first half of L3

(A-B) The genetic circuits (i) and their simulated BLMP-1, LIN-29, and UNC-5 levels (ii) in the absence (A, early to late L2 stage) or presence of DAF-12 (B, late L2 to mid L3) when the LIN-42 level is fixed, starting with a high (orange circles and arrows) or low (blue circles and arrows) UNC-5 levels. (**C-D**) Similar simulation performed in the model of different gene regulatory circuits after removing the BLMP-1 activation of *lin-29* from circuit (A) or (B).

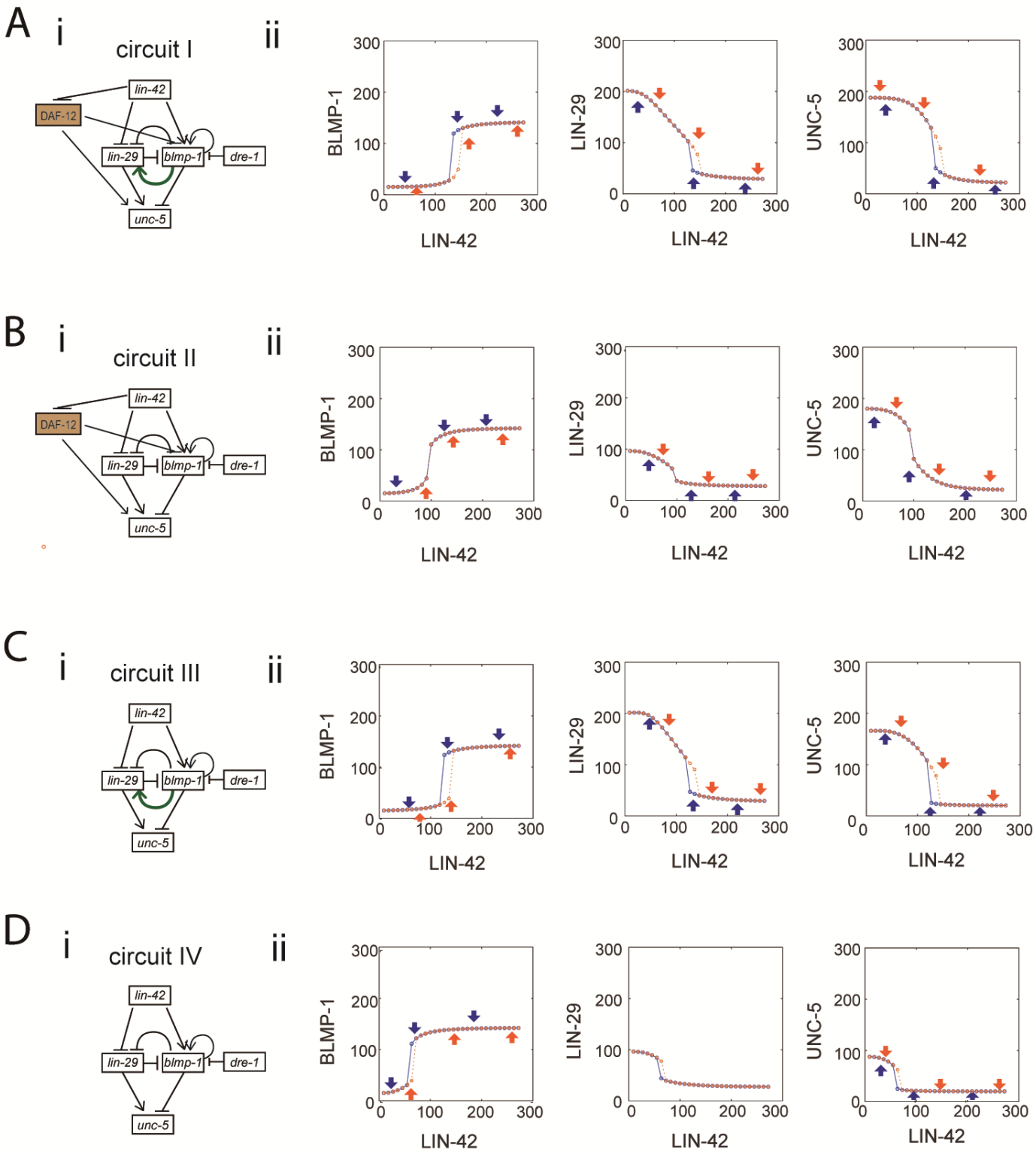

Figure S8 BLMP-1, LIN-29, and UNC-5 steady-state simulation: Response to LIN-42 levels during the second half of the LIN-42 cycle at L3 stage

(A-D) (i) The genetic circuits (I-IV) and (ii) their simulated steady state BLMP-1, LIN-29, and UNC-5 levels in the sensitized in the presence of *daf-12* (A, B) or *daf-12* mutant background (C, D, shown as a brown box), when the LIN-42 level is fixed, starting with a high (orange circles and arrows) or low (blue circles and arrows) UNC-5 levels. Gene regulatory circuits (A) and (C) include BLMP-1-mediated activation of *lin-29*, while circuits (B) and (D) are the corresponding circuits with this interaction removed.

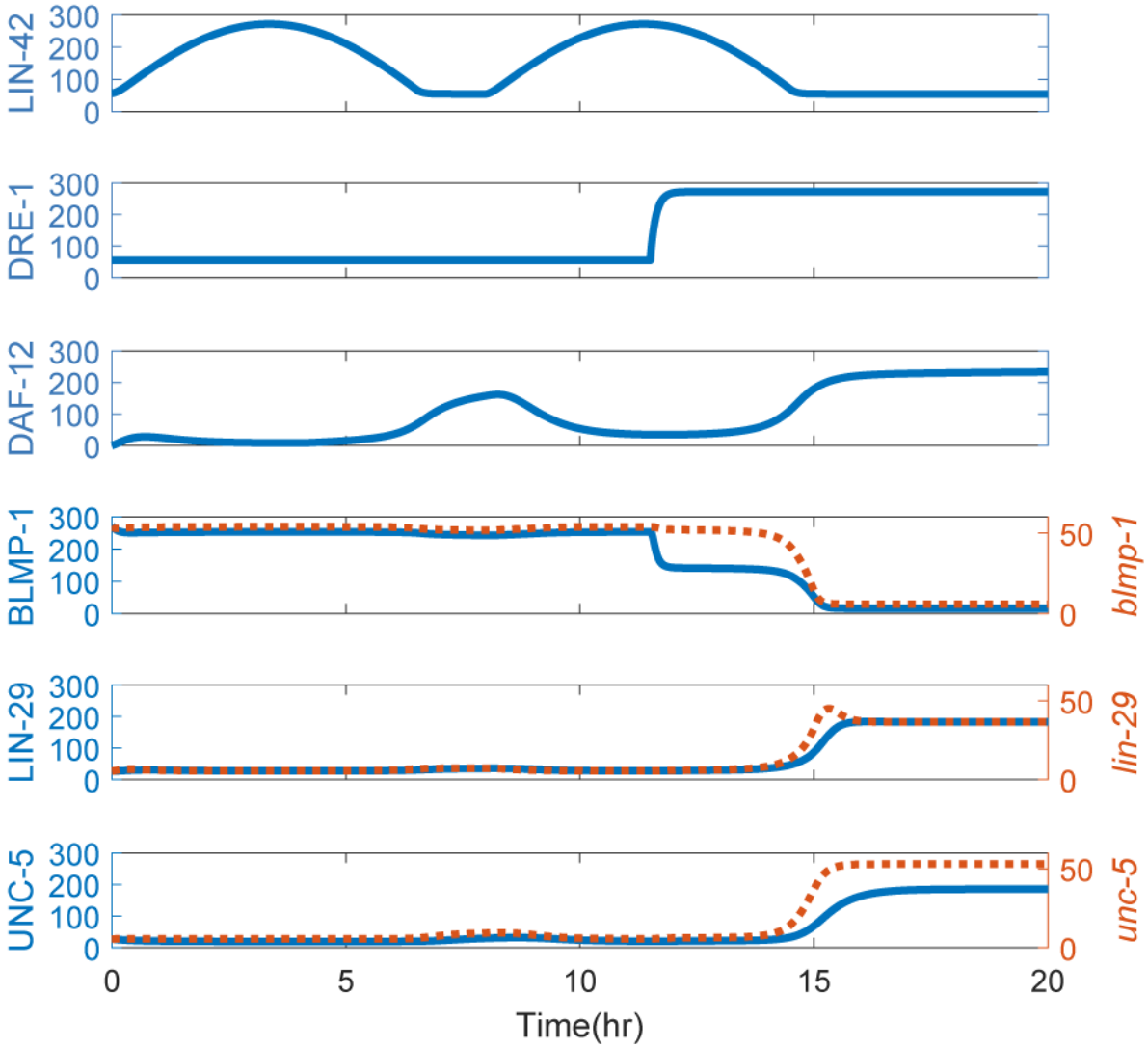

Figure S9 Deterministic simulation of BLMP-1, LIN-29, and UNC-5 expression in wild type worm.

The deterministic simulation showing how LIN-42, SCF-DRE-1, and DAF-12 regulate the mRNA and protein levels of BLMP-1, LIN-29, and UNC-5 in wild-type worms. mRNA levels are shown as red dashed lines, and protein levels are represented as solid blue lines.

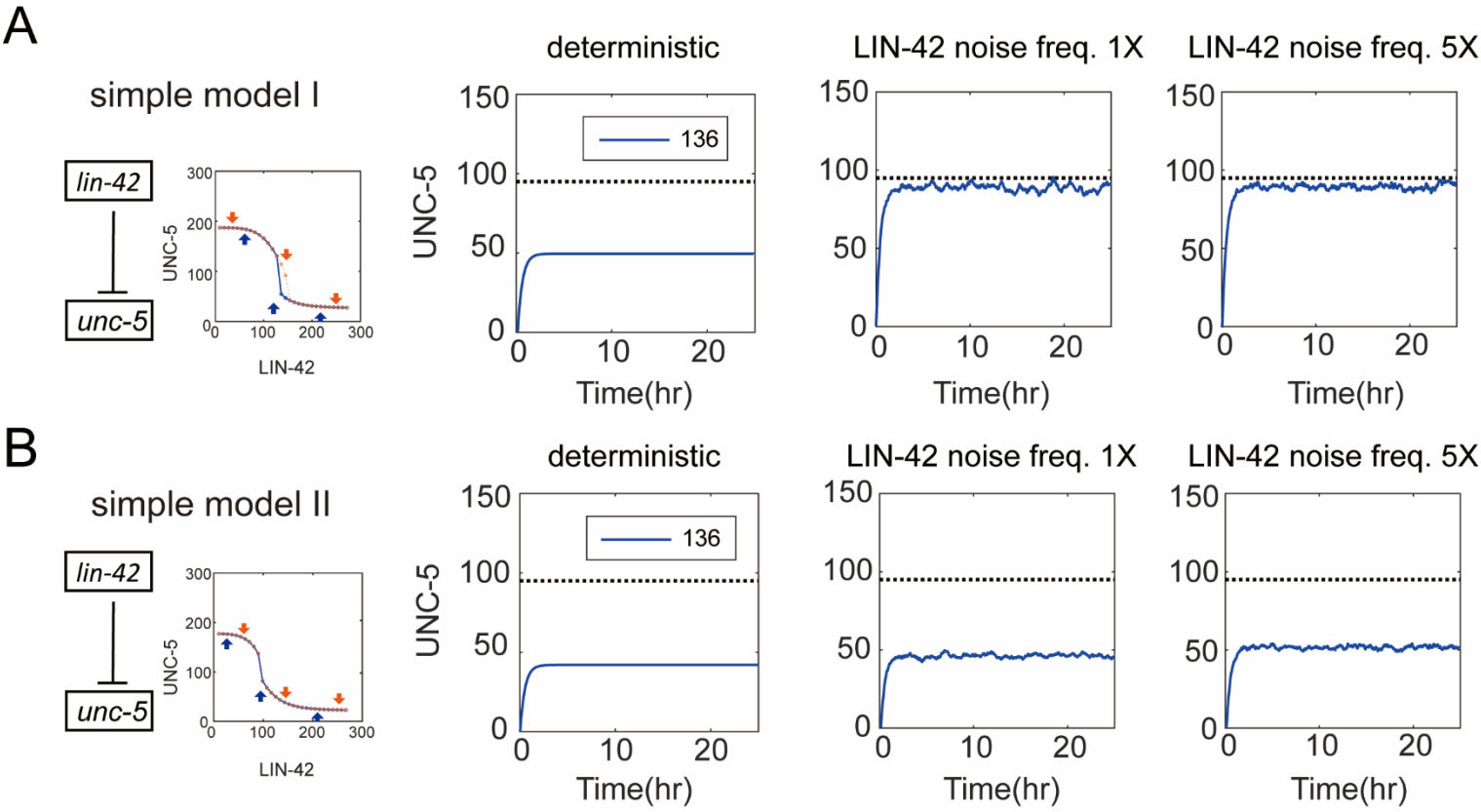

Figure S10 A simple model reproduces the noise induced switching of UNC-5 supported by BLMP-1 activation of *lin-29*.

(A-B) Based on the simple model, UNC-5 expression is directly inhibited by LIN-42. The steady-state results from circuits I (Figure S8Aii) and II (Figure S8Bii) are used to determine the regulatory function of UNC-5. Deterministic and stochastic simulation of UNC-5 reaching the steady state at indicated LIN-42 level and its noise frequency as 2154.3/hour (1X) and 10771.5/hour (5X). Each trajectory represents the mean UNC-5 level of 100 simulations

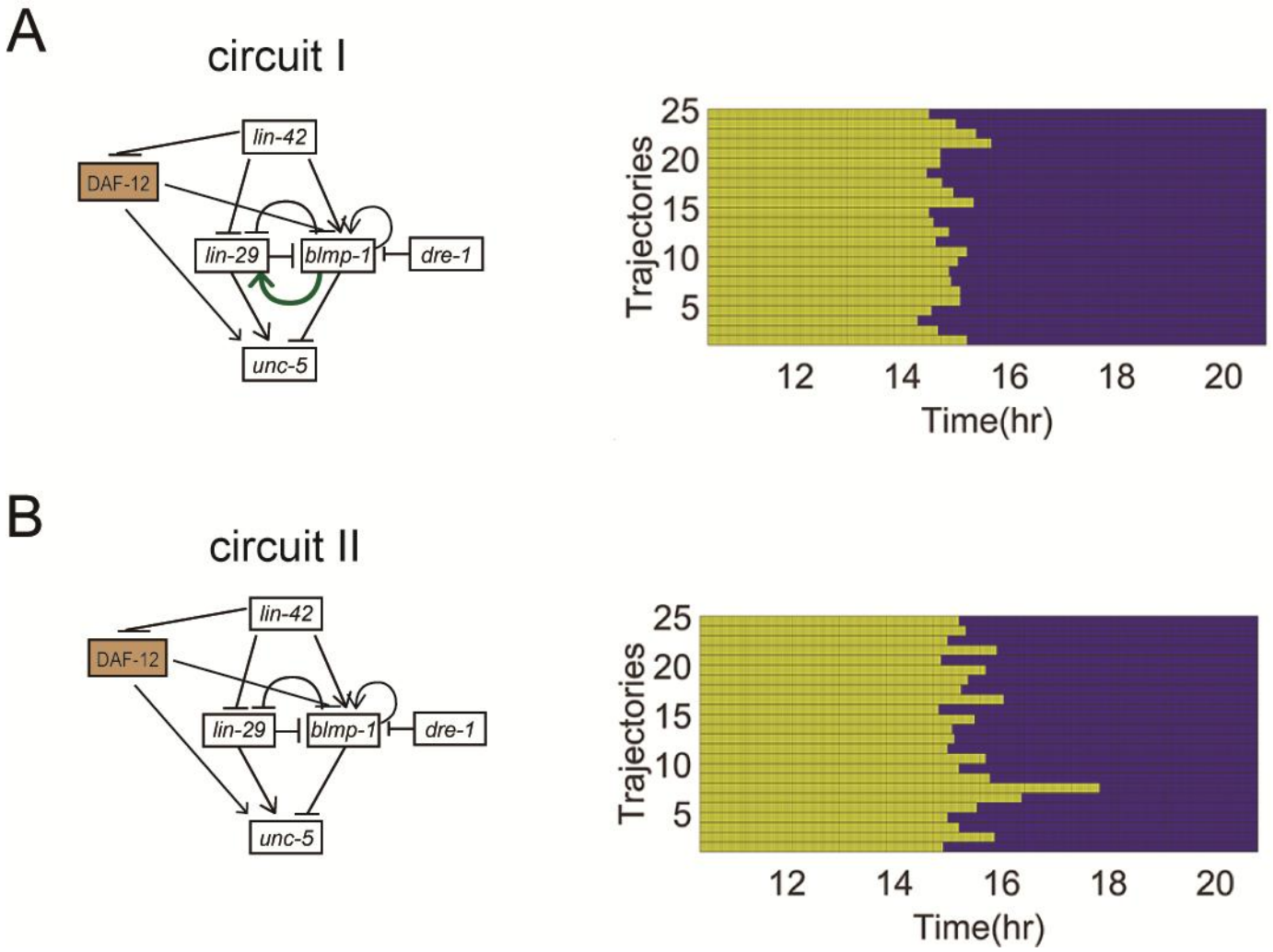

Figure S11 DTC turning pattern in the new gene regulatory circuit (A , circuit I) and the circuit lacking BLMP-1-mediated activation of *lin-29* (B, circuit II), using LIN-42 noise at a frequency of 10771.5/hour.

(A-B) (left) The gene regulatory circuits (I) and (II) in late L3 stage. (right) 25 stochastic trajectories are included with their turned (blue) or not turned (yellow) state. In these simulations cyclic LIN-42 is used as inputs to calculate the turning time.

TABLE S1 Sequence of unc-5 probes

Sequence of *unc-5* Probes	
gtgattgtgatttcgtccat	cataaccggattttggttgt
cggcattgaagacgcaatgg	tcgatccattttgagctaca
gttccgataagcttttcgat	agcgtcaatgtatccaactc
tgtgtctacgtcgattcgag	gaaaagcgtcaacgtgtcca
tctccagaagcgtaacactg	aagccacaacgtcttgatcg
aaatgaactgtcgccacgtc	atttgagaaagtgcttccgc
cttgacagggaagttggagg	tctgctttcggatctgattc
tttgcatcaggctgtacaac	ttagacttccatcagatgct
cactgtctgataatctggcg	catttgtggcttcacatgta
gtcagttttcctcgaattcg	ccaaccaccgtcaacataaa
ttgacggagaaggggacagt	cagaacgtcatgcggatcac
aagttcgtgttcttctctga	tcgttcaatggagctggatt
ttacagcttctcgtcatttc	tcctccatcaagtttacatg
actccaatcactccatgaac	cctataccgatgacaactcg
cattcatcggaggtggaacg	atctccaaaacatggctgtc
gacactcttgtgtcatcaga	gattactatccgagaggagt
ccacgtttacagcagaacat	attcattttctgcggtttca
cagaatagtagattcctcct	aatcttcgaacacctggagg
tccatgttgatgctccaaaa	gatattttctctccgagcaa
gaatgtggtagaggaggagg	cactgaatgcacttttcca
ttctaagcattgtccgtttt	ttatcgtcatccgagcaatt
agaacactcttgtcttccat	tatcaatctgcgcagcaaca
tcttgctccacttttgata	cactgccaattcaggtacaa
tgtccgaaacagccagataa	gaggtgaggttgatctgtta

TABLE S2 Sequence of *lin-29* probes

Sequence of *lin-29* Probes	
acgtccggcttttgttcgaa	aggatcaaatggatctgcgg
catctgttgctgaagcaccc	ttggattccatgagagaagt
aaggttttgcttcccgcatc	gcattatctcccattccttg
ttgacacactgcgtgcactt	gttgaaacttgacgagtcat
ataggatgagttggcaaatg	actggtctgtaagagaacta
gaattctcatgtgttgggag	agccgatcattgtattggcg
ccaaatggcttgatgccaag	gggttgtagtttgtgctctg
cttgccgcaatagttacatg	gaacgcactattctggaagg
ggtgtgatagctgagtgaac	tccgaatattaaagagctga
tgtgttcgaatgtgctgctg	gtactcggacaaatatcgat
cttatacggtttctctcctg	ctccattcttcgtactcgtc
tgtcgcatcccgtgaatttg	atgttgaacccaggagctcg
ttgcttaactgggagaatgc	gatgttctccagtggggtta
gcatcgagagtgagattgga	aagatgacccgttgtagcgt
tgaatggcttatcagtttga	gttacgacagccgtggccga
gcatttatagcaactgttac	gacgacggccgagccggtcg
agaggctctgctcgtcggtg	acgtggatgagggtgtcgat
ttgtgcttcggaatgtgatc	gacgaacctgctgacgagga
aatcttcagatgctttgact	gaacacgcctccctgacttg
ttccgcaaaacgggcaaatg	tatttatcagtgattgtggg
taagtctgttgagtgtacga	taataggaatgatttttcat
ctttgtcatgtgcttttgca	
tggccttcgatcgatccgcg	
acaacatcgtttccaaaatt	

TABLE S3 The differential equations describing the gene circuit in Figure 1Cii

$$\frac{d[\text{SCF-DRE-1}]}{dt} = \beta_p\,\theta_{\text{SCF-DRE}-1} - \gamma_p\,[\text{SCF-DRE1}], \theta_{\text{SCF-DRE}-1} = \begin{cases} 1\,, if\ t \geq 11.5 \\ \frac{1}{5}, otherwise \end{cases} \quad \text{(T1)}$$

$$\frac{d[\text{LIN-42}]}{dt} = \beta_p\,\theta_{\text{LIN}-42} - \gamma_p\,[\text{LIN-42}], \theta_{\text{LIN}-42} = \begin{cases} sin(\frac{2\pi}{15}(t\ +\ 0.5)\,, if\ t \leq 7\ and\ 8 < t \leq 15 \\ \frac{1}{5}, if\ 6.5 < t \leq 8\ and\ t > 14.5 \end{cases} \quad \text{(T2)}$$

$$\frac{d[\text{DAF-12L}]}{dt} = \beta_p\,\theta_{\text{DAF}-12\text{L}} - \gamma_{\text{DAF}-12\text{L}}\,[\text{DAF-12L}], \theta_{\text{DAF}-12\text{L}} = \begin{cases} 1\,, if\ t \geq 4 \\ \frac{1}{5}, otherwise \end{cases} \quad \text{(T3)}$$

$$\frac{d[\text{DAF12-R}]}{dt} = \beta_p\,\alpha\ + \beta_p(1-\alpha)\,g(\text{LIN-42}) - \gamma_{\text{DAF}-12\text{R}}\,[\text{DAF-12R}] \quad \text{(T4)}$$

$$\frac{d[\text{DAF-12}]}{dt} = k_{\text{DAF}-12}\,[\text{DAF12-L}][\text{DAF12-R}] - \gamma_p\,[\text{DAF12}] \quad \text{(T5)}$$

$$\frac{d[\text{X gene}]}{dt} = \beta_p\,\alpha\ + \beta_p\,(1-\alpha)\,g(\text{BLMP-1}) - \gamma_p\,[\text{X gene}] \quad \text{(T6)}$$

$$\frac{d[\textit{lin-29}]}{dt} = \beta_m\,\alpha\ + \beta_m(1-\alpha)g(\text{LIN-42})g(\text{BLMP-1})g(\text{X gene})\ \ - \gamma_m\,[\textit{lin-29}] \quad \text{(T7)}$$

$$\frac{d[\text{LIN-29}]}{dt} = \beta_p\,[\textit{lin-29}] - \gamma_{\text{LIN}-29}\,[\text{LIN-29}] \quad \text{(T8)}$$

$$\frac{d[\textit{blmp-1}]}{dt} = \beta_m\,\alpha + \beta_m(1-\alpha)(f(\text{BLMP-1}) + g(\text{LIN-42})g(\text{DAF-12})g(\text{LIN-29}) - g(\text{LIN-42})g(\text{DAF-12})g(\text{LIN-29})f(\text{BLMP-1}))\ - \gamma_m\ [\textit{blmp-1}] \quad \text{(T9)}$$

$$\frac{d[\text{BLMP-1}]}{dt} = \beta_p\,[\textit{blmp-1}] - (\,\gamma_p\ +\ Vmax_{\,\text{SCF}-\text{DRE1}\dashv\,\text{BLMP}-1}\,f(\text{SCF-DRE-1}))[\text{BLMP-1}] \quad \text{(T10)}$$

$$\frac{d[\textit{unc-5}]}{dt} = \beta_m\,\alpha\ +\ \beta_m\,(1-\alpha)(g(\text{BLMP-1})(f(\text{DAF}-12) + f(\text{LIN}-29) - f(\text{DAF}-12)f(\text{LIN}-29))\ \ -\gamma_m[\textit{unc-5}] \quad \text{(T11)}$$

$$\frac{d[\text{UNC-5}]}{dt} = \beta_p\,[\textit{unc-5}] - \gamma_{\text{UNC}-5}[\text{UNC-5}] \quad \text{(T12)}$$

where, gene *u* regulates gene *d* with the repression function g defined as,

$$g_d(u,K) = \frac{K^3_{u\dashv d}}{K^3_{u\dashv d} + u^3}\ ,$$

and the activation function *f* defined as

$$f_d(u,K) = \frac{u^3}{K^3_{u\to d} + u^3}\ .$$

TABLE S4 Parameters for deterministic simulation

Parameter	unit	values	description of the parameter
β_m / r_p	mRNA number	272	A fixed mRNA number to determine the maximum production rate of mRNA for BLMP-1, LIN-29, and UNC-5, being normalized by their respective protein degradation rates
β_p / r_p	protein number	272	A fixed protein number to determine maximum production rate of protein for LIN-42, SCF-DRE-1, DAF-12L, DAF-12R and X gene, being normalized by their respective protein degradation rates
β_p	1/hour	39.6	maximum production rate of protein for BLMP-1, LIN-29, and UNC-5
r_m	1/hour	39.6	mRNA degradation rate for *blmp-1*, *lin-29*, and *unc-5*
r_p	1/hour	7.92	protein degradation rate for all proteins except DAF-12L, DAF-12R, LIN-29 and UNC-5
$r_{\text{DAF-12L}}$	1/hour	0.24	protein degradation rate for DAF-12L
$r_{\text{DAF-12R}}$	1/hour	2.38	protein degradation rate for DAF-12R
$r_{\text{LIN-29}}$	1/hour	1.98	protein degradation rate for LIN-29
$r_{\text{UNC-5}}$	1/hour	1.98	protein degradation rate for UNC-5
$V_{\text{maxSCF-DRE-1}\dashv\text{ BLMP-1}}$	1/hour	7.2	protein degradation rate of BLMP-1 regulated by DRE-1
$k_{\text{DAF}-12}$	1/hour· protein number	0.03	binding rate between DAF-12L and DAF-12R to form DAF-12 complex
$K_{\text{DAF-12}\rightarrow \textit{unc-5}}$	protein number/per cell	130	half-activation concentration of DAF-12 to activate *unc-5* transcription
$K_{\text{LIN-29}\rightarrow \textit{unc-5}}$	protein number/per cell	110	half-activation concentration of LIN-29 to activate *unc-5* transcription

$K_{\text{BLMP-1}\dashv \textit{unc-5}}$	protein number/per cell	125	half-inactivation concentration of BLMP-1to repress *unc-5* transcription
$K_{\text{LIN-42}\dashv \textit{lin-29}}$	protein number/per cell	100	half-inactivation concentration of LIN-42 to repress *lin-29* transcription
$K_{\text{BLMP-1}\dashv \textit{lin-29}}$	protein number/per cell	85	half-inactivation concentration of BLMP-1to repress *lin-29* transcription
$K_{\text{DAF-12}\dashv \textit{blmp-1}}$	protein number/per cell	180	half-inactivation concentration of DAF-12 to repress *blmp-1* transcription
$K_{\text{LIN-42}\rightarrow \textit{blmp-1}}$	protein number/per cell	50	half-activation concentration of LIN-42 to activate *blmp-1* transcription
$K_{\text{LIN-42}\dashv \textit{DAF-12R}}$	protein number/per cell	100	half-activation concentration of LIN-42 to antagonize DAF-12 receptor activity
$K_{\text{LIN-29}\dashv \textit{blmp-1}}$	protein number/per cell	50	half-inactivation concentration of LIN-29 to repress *blmp-1* transcription
$K_{\text{BLMP-1}\rightarrow \textit{blmp-1}}$	protein number/per cell	105	half-activation concentration of BLMP-1to auto-regulate its own transcription
$K_{\text{BLMP-1}\dashv \textit{X gene}}$	protein number/per cell	15	half-inactivation concentration of BLMP-1 to repress *X* gene transcription
$K_{\text{X gene}\dashv \textit{lin-29}}$	protein number/per cell	200	half-inactivation concentration of *X gene* to repress *lin-29* transcription
$K_{\text{DRE-1}\dashv \textit{BLMP-1}}$	protein number/per cell	130	half-inactivation concentration of DRE-1 to degrade BLMP-1 protein
H		3	Hill coefficient of gene regulation function

TABLE S5 Parameters for stochastic simulation

Parameter	unit	values	description of the parameter
$a_m{}'$	none	90.7	A fixed value to determine burst frequency of transcription for BLMP-1, LIN-29, and UNC-5
b_m	mRNA number/per cell	3	burst size of transcription for BLMP-1, LIN-29, and UNC-5
a'	none	90.7	A fixed value to determine burst frequency of translation for LIN-42, SCF-DRE-1, DAF-12L, DAF-12R and X gene
b	protein number/per cell	3	burst size of translation for LIN-42, SCF-DRE-1, DAF-12L, DAF-12R and X gene

Parameter Selection Criteria

We fixed a similar maximum steady-state levels for each protein (272 molecules, Table S4), by adjusting protein production rates relative to their degradation rates (equation 30 in Materials and Methods). This adjustment allowed us to model protein dynamics based on two factors: the protein's natural degradation rate and its regulatory effects on target genes. The regulatory strength of each protein is quantified by threshold values - the concentration at which the protein achieves half of its maximum effect on its downstream targets.

In our setting, a protein degradation rate determines the time scale of its response with respect to a change. To determine such parameters, we matched gene expression and DTC turning phenotype from previous literatures and this study. For UNC-5, compared to the standard protein degradation rate (r_p) used for other proteins in the model, we assigned a slower protein degradation rate ($r_{\text{UNC-5}}$), reflecting its stable accumulation needed for gonad elongation through selective cell-matrix adhesions. This slower degradation rate allows time-averaging of noise from upstream regulators, ensuring stable UNC-5 expression for downstream events. We determined the degradation rates of DAF-12 ligand ($r_{\text{DAF-12L}}$), DAF-12 receptor ($r_{\text{DAF-12R}}$), and LIN-29($r_{\text{LIN-29}}$) by matching to the observed DTC turning times and turning time distribution in *blmp-1* and *blmp-1;daf-12* mutants. To maintain a residual BLMP-1 expression after SCF-DRE-1 mediated BLMP-1 proteolysis, we set the rate of SCF-DRE-1-mediated BLMP-1 proteolysis ($V\text{max}_{\text{SCF-DRE-1} \dashv \text{BLMP-1}}$) slightly lower than the standard protein degradation rate, which is set for BLMP-1.

Parameter	values[a]	Selection criteria the parameter
$r_{\text{UNC-5}}$	1.98	A stable accumulation of UNC-5 required for steering the motion of the elongating gonad by selectively forming cell-matrix adhesions in the direction of the turn.[1,2]
$r_{\text{DAF-12L}}$	0.24	The ligand of DAF-12, dafachronic acid was denoted as DAF-12L.Its production through DAF-9 was initiated in mid-L2[3] Its degradation rate was set by reproducing

		the precocious phenotype observed in *blmp-1* mutants, where DTC turns in early L3, as seen in Figure 1D.
$r_{\text{DAF-12R}}$	2.38	The rate was determined by the need of producing the precocious phenotype observed during early L3 stage in *blmp-1* mutants (Figure 1D).
$r_{\text{LIN-29}}$	1.98	Adjusted for reproducing experimental DTC turning time in *blmp-1;daf-12* and *blmp-1* mutants (Figure 1D).
$V\text{max}_{\text{SCF-DRE-1}\dashv\text{BLMP-1}}$	7.2	Protein degradation rate of BLMP-1 regulated by DRE-1 was set for a sufficient residual BLMP-1 for activating *lin-29*, constituting the biphasic control of BLMP-1 (Figure 1F)
r_p	7.92	Standard protein degradation rate for LIN-42, SCF-DRE-1, BLMP-1, and X gene
[a]Unit for the Protein degradation rate is 1/hour		

After determining protein-specific degradation rates, we manually selected threshold value parameters based on experimental observations. The notation and criteria for these selections are described below:

Parameter	values[a]	Selection criteria the parameter
$K_{\text{LIN-42}\rightarrow \textit{blmp-1}}$	50	A strong LIN-42 activation of *blmp-1* transcription observed in the experimental result in Figure 1E
$K_{\text{LIN-29}\dashv \textit{blmp-1}}$	50	LIN-29 strongly represses *blmp-1* transcription, as reported in the literature (Huang et al., 2014).[4]
$K_{\text{BLMP-1}\dashv \textit{lin-29}}$	85	A strong mutual inhibition between BLMP-1 and LIN-29, constituting a strong

		positive feedback loop which has been suggested crucial for cell fate transition.[4]
$K_{\text{DAF-12}\dashv \textit{blmp-1}}$	180	A weak DAF-12 repression of *blmp-1* transcription, as reported in the literature (Huang et al., 2014).[4]
$K_{\text{BLMP-1}\dashv \textit{X gene}}$	15	A low threshold makes a strong repression of X gene by BLMP-1, contributing to a strong BLMP-1 activation of *lin-29* (Figure 1F)
$K_{\text{X gene}\dashv \textit{lin-29}}$	200	A high threshold indicates weak repression of *lin-29* by the X gene. This suggests that when BLMP-1 is degraded by SCF-DRE-1, it contributes to strong BLMP-1 activation of *lin-29*, which is easily activated by the removal of the X gene's inhibitory effect (Figure 1F).
[a]Unit for the threshold values is protein number/per cell		

With these selected parameters, we validated our model by confirming it predicts both the DTC turning time and overall phenotype in wild type worms, *daf-12* mutants, and *lin-29* mutants. Our analysis determined that optimal values for the remaining regulatory threshold parameters fall within the range of 100-130 protein molecules/cell, roughly half of the maximum protein concentration (272 molecules/cell) in our simulated system. This strategic positioning of thresholds at the midpoint ensures that downstream gene regulation is responsive generally.

Parameter	Values[a]
$K_{\text{DAF-12}\rightarrow \textit{unc-5}}$	130
$K_{\text{LIN-29}\rightarrow \textit{unc-5}}$	110
$K_{\text{BLMP-1}\dashv \textit{unc-5}}$	125
$K_{\text{LIN-42}\dashv \textit{lin-29}}$	100
$K_{\text{LIN-42}\dashv \textit{DAF-12R}}$	100
$K_{\text{BLMP-1}\rightarrow \textit{blmp-1}}$	105

$K_{\text{DRE-1}\dashv BLMP\text{-}1}$	130
[a]Unit for the threshold values is protein number/per cell	

Solving for steady states of ordinary differential equations

The model, with twelve ordinary differential equations (ODEs) listed in Table S3, can be represented in the phase plane, BLMP-1 vs LIN-29, in the following way. First, we treat SCF-DRE-1 and LIN-42 as parameters, and we assume the dynamics variables described by equations (T3) -(T12) (Table S3) are in the steady state. Our goal is to express the steady-state values of these variables as functions of [BLMP-1],[LIN-29], [SCF-DRE-1] and [LIN-42].

The steady state of DAF-12 ligand [DAF-12L] and DAF-12 receptor [DAF-12R], which are obtained by setting the right-hand size of equation (T3) and (T4) to zero, can be represented by the maximum production rate (β_p) and its own degradation rate ($\gamma_{\mathrm{DAF-12L}}$), with

$$[\text{DAF-12L}] = \frac{\beta_p}{\gamma_{\mathrm{DAF-12L}}}, \tag{S1}$$

and the steady state of [DAF-12R] is described as,

$$[\text{DAF-12R}] = \frac{\beta_p}{\gamma_{\mathrm{DAF-12R}}}\alpha + \frac{\beta_p}{\gamma_{\mathrm{DAF-12R}}}(1-\alpha)g(\text{LIN-42}). \tag{S2}$$

In this equation, α represent the basal expression and the repression function (g) is as defined in Table S3.

By solving equation (T5), The DAF-12 complex [DAF-12] is represented by the binding constant ($k_{\mathrm{DAF-12}}$), [DAF-12L] and [DAF-12R], with

$$[\text{DAF-12}] = \frac{k_{\mathrm{DAF-12}}\,[\text{DAF12L}][\text{DAF12R}]}{\gamma_p} = \frac{k_{\mathrm{DAF-12}}}{\gamma_p}\frac{\beta_p}{\gamma_{\mathrm{DAF12-L}}}\frac{\beta_p}{\gamma_{\mathrm{DAF12-R}}}\alpha + \frac{k_{\mathrm{DAF-12}}}{\gamma_p}\frac{\beta_p}{\gamma_{\mathrm{DAF12-L}}}\frac{\beta_p}{\gamma_{\mathrm{DAF12-R}}}(1-\alpha)\,g(\text{LIN-42}). \tag{S3}$$

By setting the right-hand size of equation (T6) to zero, the X gene steady state is a function of BLMP-1 and represented as,

$$[\text{X gene}] = \frac{\beta_p}{\gamma_p}\alpha + \frac{\beta_p}{\gamma_p}(1-\alpha)g(\text{BLMP-1}). \tag{S4}$$

LIN-29 is the downstream of LIN-42, BLMP-1, and X gene. By setting the right-hand size of equation (T7) to zero, the steady state of *lin-29* mRNA is represented by maximum production rate of mRNA (β_m) and mRNA degradation rate (r_m), with

$$[\textit{lin-29}] = \frac{\beta_m}{\gamma_m}\alpha + \frac{\beta_m}{\gamma_m}(1-\alpha)g(\text{LIN-42})g(\text{BLMP-1})g(\text{X gene}). \tag{S5}$$

Here, we can define a LIN-29 nullcline by solving the [LIN-29] steady state of the equation (T8), with

$$[\text{LIN-29}] = \frac{\beta_p}{\gamma_{\text{LIN-29}}}\,[\textit{lin-29}] = \frac{\beta_p}{\gamma_{\text{LIN-29}}}\frac{\beta_m}{\gamma_m}\,\alpha + \frac{\beta_p}{\gamma_{\text{LIN-29}}}\frac{\beta_m}{\gamma_m}(1 - \alpha)g(\text{LIN-42})g(\text{BLMP-1})g(\text{X gene}). \tag{S6}$$

The LIN-29 nullcline can now be calculated explicitly as a function of LIN-42 and BLMP-1, from the equation (S4) for [X gene].

With the activation function (f) defined in Table S3. By solving the equation (T9), the steady state of *blmp-1* mRNA can be represented as,

$$[\textit{blmp-1}] = \frac{\beta_m}{\gamma_m}\,\alpha\, + \frac{\beta_m}{\gamma_m}\,(1-\alpha)\,(f(\text{BLMP-1}) + g(\text{LIN-42})g(\text{DAF-12})g(\text{LIN-29}) - g(\text{LIN-42})g(\text{DAF-12})g(\text{LIN-29})f(\text{BLMP-1})). \tag{S7}$$

.

This equation can be rearranged into,

$$[\textit{blmp-1}] = \frac{\beta_m}{\gamma_m}\alpha\, + \frac{\beta_m}{\gamma_m}\,(1-\alpha)\,(f(\text{BLMP-1}) + g(\text{LIN-42})g(\text{DAF-12})g(\text{LIN-29})(1 - f(\text{BLMP-1}))\,. \tag{S8}$$

The [BLMP-1] steady-state can be solved by setting the right-hand size of equation (T10) to zero, as

$$\begin{aligned}[\text{BLMP-1}] = {} & \frac{\beta_p\,[\textit{blmp-1}]}{\gamma_p + \gamma_{\text{SCF-DRE1}\dashv\ \text{BLMP-1}}\,f(\text{SCF-DRE-1})} \\ = {} & \frac{\alpha\ \beta_p\,\beta_m}{\gamma_m\ (\gamma_p\ +\ Vmax_{\text{SCF-DRE1}\dashv\ \text{BLMP-1}}\,f(\text{SCF-DRE-1}))} \\ & + \frac{\beta_p\,\beta_m}{\gamma_m\,\gamma_p\ (\gamma_p + Vmax_{\text{SCF-DRE1}\dashv\ \text{BLMP-1}}\,f(\text{SCF-DRE-1}))}\,(1 \\ & - \alpha)\,(f(\text{BLMP-1}) + g(\text{LIN-42})g(\text{DAF-12})g(\text{LIN-29})(1 - f(\text{BLMP-1}))),\end{aligned} \tag{S9}$$

where the $\gamma_{\text{SCF-DRE-1}\dashv\ \text{BLMP-1}}$ represents the BLMP-1 degradation rate mediated by SCF-DRE-1.

We multiply the items in both side of the equation by (γ_p + $\gamma_{\text{SCF-DRE-1}\dashv\ \text{BLMP-1}}\,f(\text{SCF-DRE-1})$), and the equation can be rearranged into,

$$
\begin{aligned}
[\text{BLMP-1}]\gamma_m\ (\gamma_p + Vmax_{\text{SCF-DRE1}\dashv\ \text{BLMP-1}}\, f(\text{SCF-DRE-1})) \\
= \alpha\ \beta_p\, \beta_m\ + \beta_p\, \beta_m\ (1-\alpha)\,(f(\text{BLMP-1}) \\
+ g(\text{LIN-42})g(\text{DAF-12})g(\text{LIN-29})(1-\ f(\text{BLMP-1}))\,).
\end{aligned}
\tag{S10}
$$

.

Next, we remove the item, $\alpha\ \beta_p\, \beta_m$, to left part of the equation, dividing both sides of the equation by $\beta_p\, \beta_m\ (1-\alpha)$ and the equation can be rearranged into,

$$
\begin{aligned}
&\frac{[\text{BLMP-1}]\,\gamma_m\ (\gamma_p + Vmax_{\text{SCF-DRE1}\dashv\ \text{BLMP-1}}\, f(\text{SCF-DRE-1})) - \alpha\ \beta_p\, \beta_m}{\beta_p\, \beta_m\ (1-\alpha)} \\
&= f(\text{BLMP-1}) + g(\text{LIN-42})g(\text{DAF-12})g(\text{LIN-29})(1-\ f(\text{BLMP-1}))\ .
\end{aligned}
\tag{S11}
$$

By switching the items on both side of the equation, we rearrange the equation into,

$$
\begin{aligned}
&g(\text{LIN-42})g(\text{DAF-12})g(\text{LIN-29})(1-\ f(\text{BLMP-1}))+\ f(\text{BLMP-1}) \\
&= \frac{[\text{BLMP-1}]\,\gamma_m\ (\gamma_p + Vmax_{\text{SCF-DRE1}\dashv\ \text{BLMP-1}}\, f(\text{SCF-DRE-1})) - \alpha\ \beta_p\, \beta_m}{\beta_p\, \beta_m\ (1-\alpha)}\ .
\end{aligned}
\tag{S12}
$$

We isolate $g(\text{LIN-29})$, which can be represented as $\frac{K^3_{\text{LIN-29}\dashv\ blmp1}}{K^3_{\text{LIN-29}\dashv\ blmp1} + [\text{LIN-29}]^3}$, to the left part of the equation, moving all the other terms to the right part of the equation, and the equation can be rearranged into,

$$
\begin{aligned}
&\frac{K^3_{\text{LIN-29}\dashv\ blmp-1}}{K^3_{\text{LIN-29}\dashv\ blmp-1}\ +\ [\text{LIN}-29]^3} \\
&= \frac{\dfrac{[\text{BLMP-1}]\,\gamma_m\ (\gamma_p + Vmax_{\text{SCF-DRE1}\dashv\ \text{BLMP-1}}\, f(\text{SCF-DRE-1})) - \alpha\ \beta_p\, \beta_m}{\beta_p\, \beta_m\ (1-\alpha)}\ - f(\text{BLMP-1})}{g(\text{LIN-42})g(\text{DAF-12})(1-\ f(\text{BLMP-1}))}\ .
\end{aligned}
\tag{S13}
$$

After switching numerator and denominator, we rearrange the equation into,

$$
\begin{aligned}
&\frac{K^3_{\text{LIN-29}\dashv\ blmp-1}\ +\ [\text{LIN}-29]^3}{K^3_{\text{LIN-29}\dashv\ blmp-1}} \\
&= \frac{g(\text{LIN-42})g(\text{DAF-12})(1-\ f(\text{BLMP-1}))}{\dfrac{[\text{BLMP-1}]\,\gamma_m\ (\gamma_p + Vmax_{\text{SCF-DRE1}\dashv\ \text{BLMP-1}}\, f(\text{SCF-DRE-1})) - \alpha\ \beta_p\, \beta_m}{\beta_p\, \beta_m\ (1-\alpha)}\ - f(\text{BLMP-1})}\ .
\end{aligned}
\tag{S14}
$$

The equation can be represented as,

$$[\text{LIN}-29]^3 = \frac{K^3_{\text{LIN}-29 \dashv blmp-1}\, g(\text{LIN-42}) g(\text{DAF-12})(1 - f(\text{BLMP-1}))}{\frac{[\text{BLMP-1}]\,\gamma_m\,(\gamma_p + Vmax_{\text{SCF}-\text{DRE1}\dashv\,\text{BLMP}-1} f(\text{SCF-DRE-1})) - \alpha\,\beta_p\,\beta_m}{\beta_p\,\beta_m\,(1-\alpha)} - f(\text{BLMP-1})} - K^3_{\text{LIN}-29 \dashv blmp-1} \quad \text{(S15)}$$

Now the second nullcline, from solving the BLMP-1 steady state (equation (T10) in Table S3) can be derived from equation (S15), where the [LIN-29] is a function of LIN-42 and BLMP-1, from the equation (S3) for [DAF-12].

By setting the right-hand size of equation (T11) and (T12) to zero, *unc-5* mRNA and UNC-5 steady-state are represented as,

$$[unc\text{-}5] = \frac{\beta_m}{\gamma_m}\,\alpha + \frac{\beta_m}{\gamma_m}(1-\alpha)(g(\text{BLMP-1})(f(\text{DAF}-12) + f(\text{LIN}-29) - f(\text{DAF}-12) f(\text{LIN}-29)), \quad \text{(S16)}$$

and

$$[\text{UNC-5}] = \frac{\beta_\text{p}}{\gamma_{\text{UNC}-5}}[unc\text{-}5] = \frac{\beta_\text{p}}{\gamma_{\text{UNC}-5}}\frac{\beta_m}{\gamma_m}\,\alpha + \frac{\beta_\text{p}}{\gamma_{\text{UNC}-5}}\frac{\beta_m}{\gamma_m}(1-\alpha)(g(\text{BLMP-1})(f(\text{DAF}-12) + f(\text{LIN}-29) - f(\text{DAF}-12) f(\text{LIN}-29)), \quad \text{(S17)}$$

where $f(\text{DAF}-12)$ is a function of LIN-42, from the equation (S3) for [DAF-12].

References

1. Agarwal, P., Shemesh, T. & Zaidel-Bar, R. Directed cell invasion and asymmetric adhesion drive tissue elongation and turning in *C. elegans* gonad morphogenesis. *Developmental Cell* **57**, 2111-2126.e6 (2022).
2. Cecchetelli, A. D. & Cram, E. J. Regulating distal tip cell migration in space and time. *Mechanisms of Development* **148**, 11–17 (2017).
3. Jia, K., Albert, P. S. & Riddle, D. L. DAF-9, a cytochrome P450 regulating C. elegans larval development and adult longevity. *Development* **129**, 221–231 (2002).
4. Huang, T.-F. *et al.* BLMP-1/Blimp-1 Regulates the Spatiotemporal Cell Migration Pattern in C. elegans. *PLOS Genetics* **10**, e1004428 (2014).